Laser interferometer for measuring high velocities of any reflecting surface*

L. M. Barker and R. E. Hollenbach
Shock-Wave Phenomena Division 5163, Sandia Laboratories, Albuquerque, New Mexico 87115
(Received 28 April 1972)

A laser velocity interferometer instrumentation system has been developed which can measure the velocity history of either spectrally or diffusely reflecting surfaces. The system provides two interferometer fringe signals in quadrature to improve resolution and to distinguish between acceleration and deceleration. Accuracies of 2% or better are attainable for peak surface velocities of 0.2 mm/μsec or more. The system has been applied to the measurement of free surface motion in plate-impact experiments, and to the measurement of the velocity history of a projectile during its acceleration down a long gun barrel.

I. INTRODUCTION

Laser interferometry has become generally accepted as a precision tool for obtaining velocity-vs-time profiles of the motion of the surfaces of shocked specimens.[1] However, most interferometer techniques have required (a) specimen surfaces which retain a mirror finish and (b) very little specimen surface tilt during the motion of interest. These requirements have either complicated or precluded the use of interferometry in a wide range of shock instrumentation problems.

The velocity interferometer instrumentation system described here retains the 1–2% accuracies of previous techniques[2,3] while monitoring the motion of either spectrally or diffusely reflecting surfaces, or of surfaces which are neither perfectly spectral nor perfectly diffuse. The new system has been called a "velocity interferometer system for any reflector" (VISAR). It is by its nature also quite insensitive to tilting of the specimen surface during the experiment, especially when a diffuse specimen surface is used. Thus, the VISAR is expected to greatly expand the usefulness of interferometry in shock-wave research at very high shock pressures for porous, composite, and geological materials and in multiaxial wave experiments. The VISAR can also be used in a mode which provides a very large depth of field, such that, for example, the velocity history of a projectile during its acceleration from the breech to the muzzle of a long gun barrel can be accurately measured.

This paper describes the new interferometer instrumentation system, presents some of the first measurements made with the device, and discusses the factors contributing to its accuracy.

II. BACKGROUND

The Sandia laser velocity interferometer (Fig. 1) is probably the most widely used interferometer configuration for shock profile measurements. It uses a laser light beam which is reflected from a mirrorized surface of a shocked specimen. The beam is then split, and part of it is delayed (usually by a few nsec) before being recombined with the undelayed portion of the beam. Thus, the light frequency consisting of the laser light frequency plus the Doppler shift imparted by the moving specimen surface is constantly being combined with the light frequency which existed a short time τ earlier, where τ is the delay time.

A derivation is given in Ref. 2 which relates the fringe count $F(t)$ to the specimen surface velocity $u(t-\frac{1}{2}\tau)$:

$$u(t-\tfrac{1}{2}\tau)=\frac{\lambda F(t)}{2\tau(1+\Delta\nu/\nu_0)}. \tag{1}$$

Here, t is time, λ is the wavelength of the laser light, and $\Delta\nu/\nu_0$ is an index-of-refraction correction factor which is equal to zero unless a "window" material[2] is placed on the specimen's reflective surface.

Unfortunately, being a long path length difference interferometer, the velocity interferometer of Fig. 1 requires a good mirror finish on the specimen surface so that spatial coherence of the laser beam is maintained on reflection. A displacement interferometer[3] also requires a good mirror specimen surface, since that surface is one of the two mirrors in a Michelson interferometer. However, it is well known that spatially incoherent light (such as laser light which has been reflected from a diffuse surface) can be used as the *incident* beam on a Michelson interferometer, provided that the two legs of the interferometer are nearly the same length. Thus, one might illuminate the Michelson interferometer of Fig. 2(a) with the Doppler-shifted light from either a spectrally or a diffusely reflecting specimen surface. Good fringe contrast could be obtained, but no motion would be detected because neither of the mirrors *in* the interferometer would move. Or, if viewed as a velocity interferometer, no motion would be detected because the difference in transit times of the light through the two legs of the interferometer is zero. With τ equal to zero, it follows from Eq. (1) that the fringe count must also remain equal to zero for all finite velocities.

What is needed is a modification to the interferometer of Fig. 2(a) such that the two legs of the interferometer appear equal, yet such that the light in one of the legs is delayed with respect to the light in the other leg. These

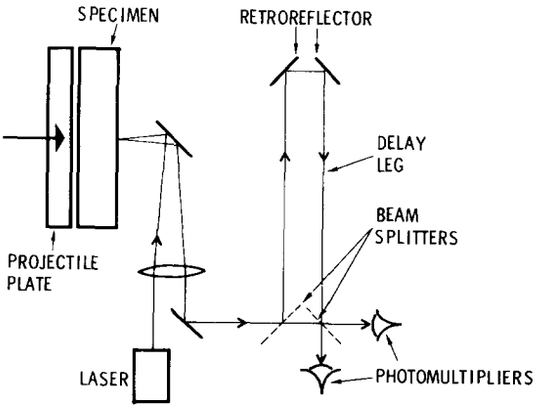

FIG. 1. Sandia velocity interferometer—this configuration is widely used for shock profile measurements, but it requires that the specimen surface retain a good mirror finish during the experiment.

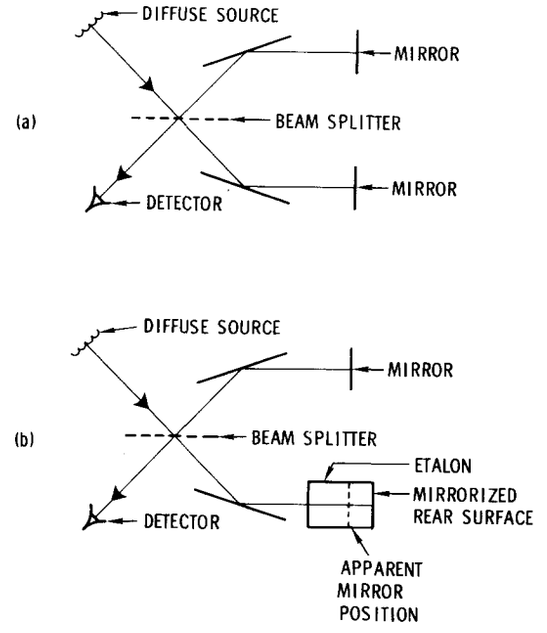

FIG. 2. Michelson and WAMI—a Michelson interferometer with equal leg lengths is shown in (a). The configuration shown in (b) is such that the two legs of the interferometer appear to the detector to be equal, yet it takes longer for light to traverse the leg containing the etalon.

seemingly contradictory requirements are met with the so-called wide-angle Michelson interferometer (WAMI)[4] configuration of Fig. 2(b). The apparent position of the mirrorized rear surface of the transparent etalon, as viewed by the detector, is closer to the beam splitter than the actual mirrorized surface by an amount[4]

$$x = h(1 - 1/n), \tag{2}$$

where h is the length of the etalon and n is its index of refraction. If the apparent mirror position is placed at the same distance from the beam splitter as the mirror in the other leg of the interferometer, spatial coherence of the light is not required, and very good fringe contrast can be obtained even with light reflected from a diffuse surface. The light in the leg containing the etalon is delayed with respect to the light in the other leg because it has farther to travel and because it travels slower in the etalon material. It is not difficult to show that the delay time is given by[4]

$$\tau = (2h/c)(n - 1/n), \tag{3}$$

where c is the velocity of light in free space. Thus, the velocity interferometer Eq. (1) applies, and the WAMI can be used as a velocity interferometer for any reflecting surface.

The WAMI was described in the literature as early as 1941.[5] It has the property of enlarging the acceptance angle of the Michelson interferometer, i.e., of enlarging the field of view for which an all-dark or an all-light fringe pattern can be obtained.[4] The WAMI has therefore proved useful in cases where the source is broad and of low light level, such as the nightglow and the aurora.[6]

The WAMI was first used as a velocity interferometer by Gillard.[7,8] However, to the authors' knowledge, Gillard's "velocimeter" was never adapted outside his own organization, and it is now no longer in use.[9] The VISAR described below is another adaptation of the WAMI for use as a velocity interferometer. The VISAR configuration contains several features which give it an accuracy advantage over Gillard's velocimeter, and which make its precision comparable to that of the Sandia velocity interferometer.

III. VISAR

A schematic of the interferometer section of the VISAR instrumentation system is shown in Fig. 3. The incident light beam has been collected from the laser light reflected from the surface of a specimen, and hence already contains the Doppler shift resulting from the surface motion. The beam is incident at a few degrees from the normal on one part of the large beam splitter (63-mm diameter). The reflected part of the beam is returned by the mirror M1 to a different part of the large beam splitter, where it is recombined with the initially transmitted part of the incident beam. At the time of the recombination, the transmitted part of the beam has been delayed with respect to the reflected beam by one or more etalons in the right-hand leg of the interferometer. The substrate of the large beam splitter must be considered as an etalon since it is not balanced by an equal thickness of material on the left of the beam-splitting surface. The amount of the delay attributable to each etalon is given by Eq. (3), where h is the effective length of the etalon. The effective length is slightly longer than the physical length because the light travels through the etalon at a small angle to the longitudinal axis. There is also a slight delay due to the presence of the quarter-wave plate, whose function is described below. Only one-half of the thickness of the quarter-wave plate is used in calculating its contribution to the total delay, because the transmitted beam passes through it only once.

The mirror M2 of the interferometer is adjustable in angular orientation to facilitate alignment of the interferometer. Its distance from the beam splitter is also adjustable to accommodate the various etalon lengths which may be required. The distance of M2 from the beam splitter is equal to the distance of M1, plus the sum of the x's given by Eq. (2) for each etalon.

The mirror M1 is mounted on a piezoelectric translator about 30 cm from the large beam splitter (Fig. 3). The

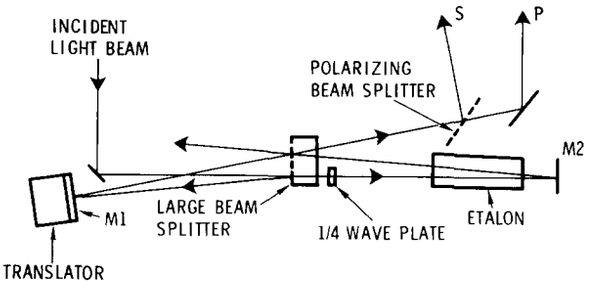

FIG. 3. VISAR interferometer.

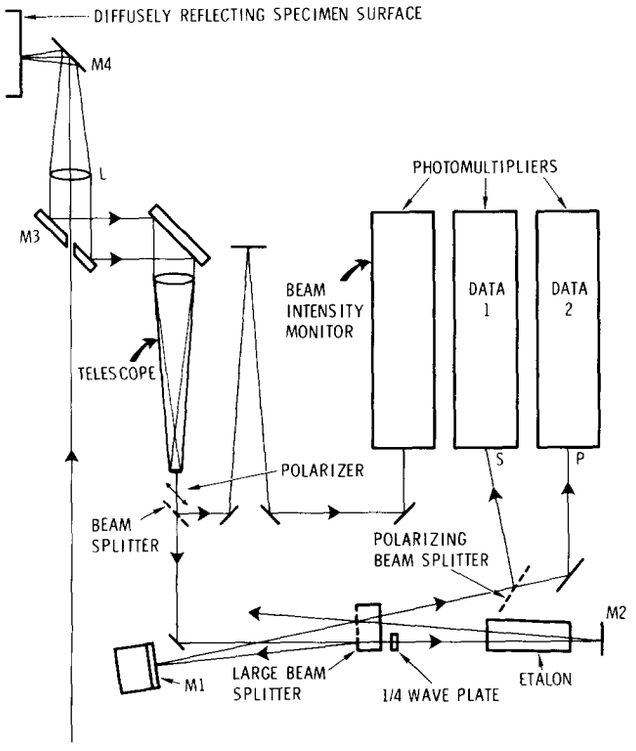

FIG. 4. Schematic of the VISAR instrumentation system—except for the lens L, the mirror M4, and the specimen, all of the components shown here are permanently mounted on a special roll table which provides mobility and minimizes the optical alignment time. The laser, its power supply, and the photomultiplier power supplies are also located in the roll table.

translator varies the length of the left-hand leg of the interferometer by a few wavelengths of light as the voltage to the translator is varied. This feature allows one to produce a few fringes by varying a potentiometer setting, which is a convenience for the alignment of the interferometer, for subsequent checking of the alignment and fringe contrast, and for setting the deflection sensitivities of the recording oscilloscopes.

All of the surfaces of the optics in the interferometer are flat to $\frac{1}{20}\lambda$. The etalons are made of Schlieren-grade fused silica with less than $\frac{1}{10}\lambda$ distortion of the wave front. Low-loss dielectric coatings are used on all surfaces to enhance the desired transmission or reflection properties.

The individual etalons have lengths up to 10 cm. As many as five etalons at a time (in addition to the beam splitter and the $\frac{1}{4}\lambda$ plate) have been used to achieve a total of 32 cm of etalon material in the delay leg. The resulting delay time was over 1.6 nsec. Although much longer delays are theoretically attainable simply by inserting more etalons into the delay leg, practical considerations will generally limit the delay to a fraction of that normally used in the Sandia velocity interferometer. Thus, instead of having the peak measured velocity correspond to a fringe count of 5—10, the fringe count may be only 1—2 fringes for the VISAR. In order to attain comparable velocity resolution, it therefore is necessary to decrease the error in determining the fringe count at any given time.

One feature incorporated into the VISAR for improving its accuracy is the simultaneous monitoring of two fringe signals which are 90° out of phase. These signals are obtained in quadrature by the method of Bouricious and Clifford[10] where the incident light beam is polarized at 45° to the vertical, such that it consists of half-S and half-P polarized light. The quarter-wave plate (Fig. 3) is arranged to retard the P component of the light by a phase angle of 90° with respect to the S component of the transmitted beam. Thus, when the recombination occurs at the beam splitter, the S and P components form two 90°-out-of-phase fringe patterns. The two patterns are separated from each other by the polarizing beam splitter and are then sent to their individual photodetectors.

In order to optimize the performance of the interferometer, it is desirable to have the large beam splitter transmit and reflect 50% of the incident light of both S and P polarizations. However, for most beam splitters the S and P reflectances differ progressively as the angle of incidence increases. The VISAR interferometer was therefore designed such that the angles of incidence of the light beams onto the large beam splitter are only a few degrees from the normal, thus assuring nearly equal reflectances for the S and P polarized components.

The advantage of recording two signals which are 90° out of phase can be appreciated by noting that a plot of the interferometer's output light intensity I vs the fringe count F is simply a sine wave. Thus, $dI/dF = 0$ at intensity maxima and minima. This means that a slight change in the fringe count is not accompanied by a detectable change in the output light intensity whenever the intensity is passing through a maximum or a minimum value. The maxima and minima of a given fringe record therefore represent points of poor resolution of the fringe count. Having two fringe records which are 90° out of phase solves this problem because one or the other of the signals will always be in a region of good resolution. A second benefit of 90°-out-of-phase signals is that acceleration can be distinguished from deceleration, for in the first case one of the signals leads the other by 90°, whereas in the second it lags by 90°. One signal or two signals 180° out of phase are by themselves ambiguous, for acceleration and deceleration are indistinguishable, as are reversals in acceleration which occur near fringe maxima or minima.

A schematic of the complete VISAR instrumentation system is presented in Fig. 4, where a diffusely reflecting specimen surface is assumed. The ingoing laser beam passes through a small hole in the mirror M3 and then through the 50-mm-diam focusing lens L. The mirror M4 directs the beam onto the specimen surface, which is at the focal point of the lens L. The mirror M4 then illuminates lens L with the diffusely reflected light if a diffuse reflecting surface is used or it returns the reflected light beam to an off-center position on lens L if a spectral specimen surface is used. The lens L recollimates the reflected light for use in the interferometer. The mirror M3 separates the reflected beam from the incident beam, and, in the case of a diffuse specimen surface, the telescope condenses the reflected beam to a convenient diameter for use in the interferometer (about 7 mm). In the case of a spectral specimen surface, the

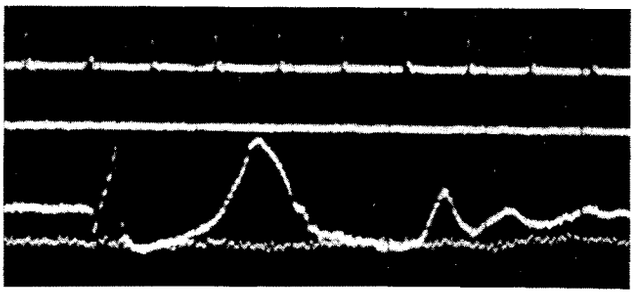

FIG. 5. Oscillogram of the iron impact experiment. At the top is a 5-MHz timing trace. Second is the zero-light baseline for both photomultipliers. The positive light direction is downward. The third trace is the signal from one of the two data photomultipliers, and the fourth trace is from the beam-intensity monitor.

telescope localizes the reflected beam to within a 7-mm diameter for transmission through the rest of the optics. Following the telescope, a polarizer assures that the light is polarized at 45° from the horizontal to give the equal intensities of S and P light required by the interferometer.

About one-third of the light is then split away from the main beam and directed to the beam-intensity monitor photomultiplier tube (Fig. 4). The purpose of the beam-intensity monitor is to detect any change in the intensity of the light reflected from the specimen surface. Intensity changes are caused mainly by shock-induced changes in surface reflectivity. By providing a record of the beam intensity vs time, the beam-intensity monitor makes it possible to correct the interferometer data for any variations in beam intensity. Notice that the light for the beam-intensity monitor is sent around a delay path en route to its photomultiplier. Without such a delay, the longer light paths to the data photomultipliers would cause the data signals to be slightly out of synchronization with the beam-intensity signal.

Because of the unequal splitting of S and P components of polarized light by beam splitters, the beam splitter which provides the beam-intensity monitor light can alter the 45° polarization of the incident light. This problem was overcome by tilting the beam splitter such that the reflected beam goes upward at an angle of 45° with the horizontal. In this position, the 45° polarized light is all S polarized with respect to the beam splitter, and the polarization angle is therefore unaltered on transmission. A small mirror next to the beam splitter (not shown in Fig. 4) brings the reflected beam back to the horizontal direction.

The operation of the interferometer portion of the VISAR has already been explained. The beam-intensity signal and the two 90°-out-of-phase fringe signals from the interferometer are sensed by three RCA C 7291D photomultiplier tubes with a current gain of about 10^4 and less then 2-nsec rise time. The data are recorded with dual-beam oscilloscopes. One trace on each scope shows the variation of the beam intensity, while the other trace shows the signal from one of the fringe-sensing photomultipliers.

The only remaining component of the VISAR which has not been discussed is the laser light source. Although spatially coherent light is not necessary in the VISAR interferometer, very good temporal coherence *is* required because one of the two interfering beams may be delayed with respect to the other by nearly 10^6 light-frequency periods. Thus, one should use a laser operating at a single frequency, i.e., in a single longitudinal as well as single transverse mode. The laser light power required depends strongly on the reflection characteristics of the specimen surface, including its reflection coefficient and whether it is primarily a diffuse or a spectral surface. The photomultipliers need 10—30 μW of power to give reasonably good signal-to-noise ratios. Thus, a 200-μW laser power is sufficient when a spectral specimen surface of high reflectivity is used, whereas 0.1 W or more may be needed for diffuse surfaces of poor reflectivity. Fortunately, cw lasers providing at least 0.4 W of single-frequency power are now commercially available.

IV. DATA AND RESULTS

Only a few experiments have been done using the VISAR, and although they were performed without the benefit of the much higher laser power available in ion lasers, they nevertheless demonstrated the VISAR's accuracy and flexibility. Two of the early experiments are described below. With the incorporation of an ion laser, and with other improvements which derive partly from experience in using the system, even better experimental results can be expected in the future.

In the first experiment the objective was to measure the free-surface velocity profile of an Armco iron specimen after an impact which produced a peak stress of about 170 kbar. Of special interest was the shape of the velocity profile corresponding to the phase transition wave[11] above 130 kbar. Earlier attempts to measure this portion of the velocity history using the Sandia velocity interferometer have failed, apparently because the arrival of the phase transition wave ruined the mirror surface on the iron.

The projectile nose piece was a 3.36-mm-thick disk of tungsten carbide of density 14.7 g/cm^3. The impact velocity was 0.615 mm/μsec. The specimen was a 3.11-mm-thick disk of Armco iron with a diffusely reflecting free surface which had been lapped but not polished. One of the oscillograms of the VISAR data is shown in Fig. 5. The fine structure on the data traces is attributed partly to shot noise in the photomultiplier. The shot noise should vary as the inverse root of the laser power, and hence should decrease markedly with the use of a high-power ion laser. Part of the fringe signal occurred at too high a frequency to be followed by the 50-MHz bandwidth oscilloscopes and thus, the fringe count was at first uncertain beyond the high-frequency region. However, the fringe levels corresponding to zero velocity and to the peak velocity reveal that the fringe count at the peak velocity is $n+0.16$, where n is an integer. It is easily determined from the boundary conditions of the experiment that $n=4$.

The reduced data from the iron experiment are shown in Fig. 6. Much of the measured velocity history could not

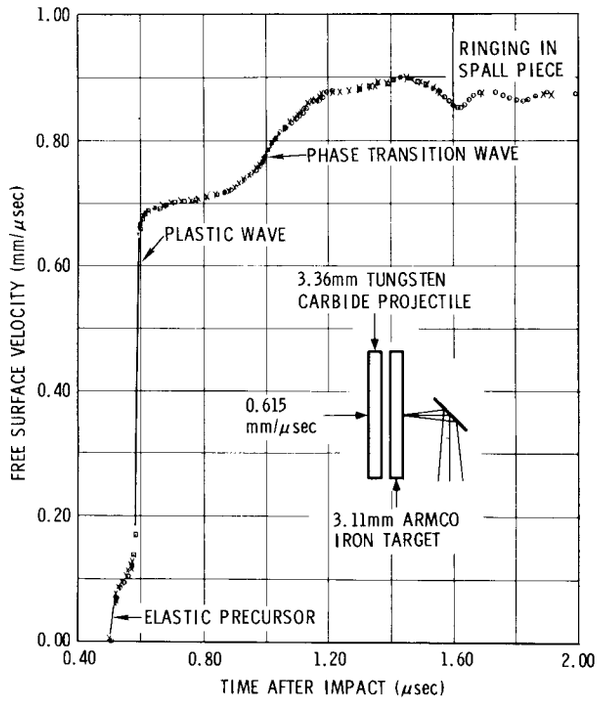

FIG. 6. Reduced data from the iron experiment—inset shows the impact configuration. The velocity profile is computer plotted, and shows the data points read from four oscillograms of the interferometer output.

have been obtained by an interferometer requiring a spectral specimen surface. In the first place, as mentioned above, the phase transition wave ruins a mirror surface. Second, the later oscillations in velocity are due to the ringing of a layer of iron which was spalled off from the rest of the specimen, and experience has shown that the occurrence of spall results in the destruction of the free-surface mirror. Finally, good data were obtained well beyond the time of arrival of edge effects at the measuring point and, again, experience has shown that edge effects ruin a mirror surface. Thus, the ability and the value of being able to monitor a diffusely reflecting specimen surface was conclusively demonstrated in this experiment.

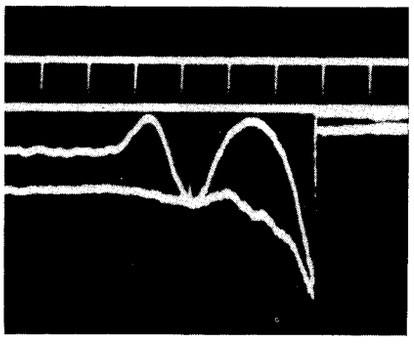

FIG. 7. Projectile acceleration measurement experiment—trace identifications are the same as for Fig. 5. The time mark frequency is 200 Hz in this oscillogram.

The objective of the second experiment was to measure the velocity history of a 10-cm-diam projectile during its acceleration from the breech to the muzzle of a 4-m-long gun barrel. A 2.5-cm square of Scotchlite tape was attached to the center of the projectile nose plate to reflect the incident laser beam. The tape acts as a diffuse reflector, but the reflected light is highly concentrated in the direction of the incoming beam. Thus, sufficient light for the experiment was reflected back onto the telescope objective. The lens L of Fig. 4 was removed for this experiment, and the light path length between mirrors M3 at the VISAR and M4 at the muzzle of the gun was lengthened to about 10 m. The laser-beam diameter at the projectile nose was about 5 mm. The reflected light entering the telescope was very nearly collimated because of the large distance from the projectile nose to the telescope. The rest of the VISAR configuration remained as shown in Fig. 4.

One of the oscillograms of the data is shown in Fig. 7. The beam-intensity monitor trace shows an increase in the light level as the projectile comes down the barrel. This is caused by the decrease in the inverse-square attenuation of the light as the distance from the projectile to the telescope objective decreases. The fringe frequency is much more nearly constant than it was for the iron experiment because of the more constant acceleration of the reflecting surface. The light levels drop to zero when the projectile impacts the mirror M4 at the muzzle of the gun. The measured velocity history from this experiment is shown in Fig. 8.

V. DISCUSSION OF ACCURACY

The VISAR data reduction assumes that the fringe amplitude at time t on the oscillogram is a sinusoidal function of the fringe count at time t [12]:

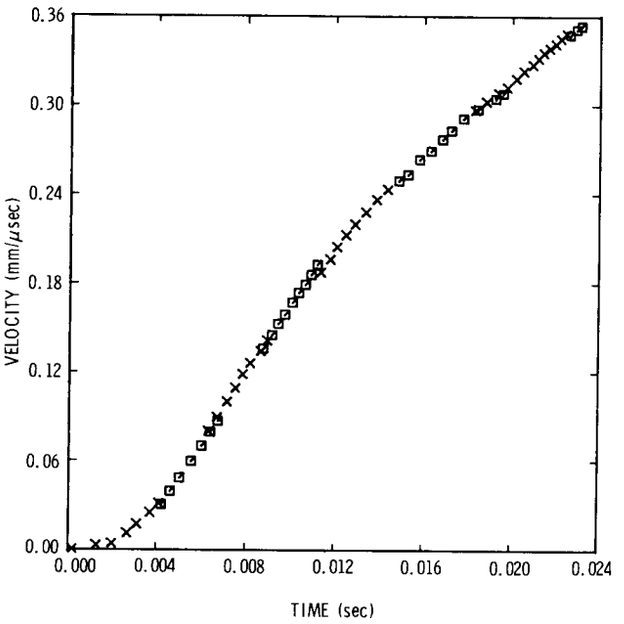

FIG. 8. Projectile velocity vs time—two different symbols in the graph are used for plotting the data from the two 90°-out-of-phase signals from the interferometer.

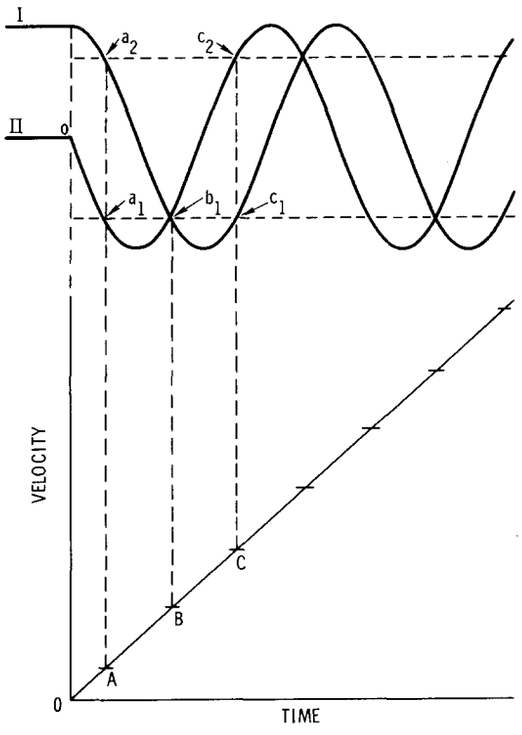

FIG. 9. VISAR data-reduction procedure.

$$A(t) = \tfrac{1}{2}A_{max}\{1 + \sin[2\pi F(t) + \delta]\}, \quad (4)$$

where A_{max} is the fringe-peak–to–fringe-trough excursion and δ is the phase angle determined by the amplitude corresponding to zero velocity. This equation can be solved for $F(t)$, and the surface velocity can then be obtained from Eq. (1). The value of A_{max} varies with the intensity of the light coming through the telescope of Fig. 4. The value of A_{max} as a function of the time is therefore determined from the beam-intensity monitor record.

The assumption that $A(t)$ is related to $F(t)$ by Eq. (4) is imperfect because of the presence of shot noise in the photomultiplier outputs, slight nonlinearities of the photomultipliers and oscilloscopes, and finite rise times of the electronics, for example. The shot noise problem should be decreased significantly by the use of a much more powerful argon-ion laser. The linearity of the system has been measured and is better than 3%. Nevertheless, in view of these uncertainties, and inasmuch as the oscillograms of Figs. 5 and 7 are much less than outstanding in appearance, the reader may logically question any claim of 2% accuracy of data reduced from such oscillograms.

The key to the accuracy of the VISAR lies in the fact that it essentially magnifies the recording of the velocity when the peak velocity is large enough to produce one or more fringes. For most transducers the maximum vertical deflection on an oscillogram corresponds to the maximum excursion of the measured parameter. However, with the VISAR, 70% of the maximum vertical deflection may typically correspond to only about 10% of the maximum excursion in velocity. Thus, any noise or erroneous deflections on the data trace are strongly demagnified (by a factor of about 7 in this example) in the final plot of the data. The reason for this effect is illustrated in the drawings of Fig. 9, where the two 90°-out-of-phase signals at the top are the idealized interferometer outputs which would result from the linearly increasing velocity shown in the graph. Having obtained the oscillograms of the interferometer output, one would retrieve the velocity versus time by taking readings on data trace II from o to a_1. This defines the velocity from 0 to A. Readings would then be taken on data trace I from a_2 to b_1, which gives the velocity from A to B. The next readings would be taken on data trace II from b_1 to c_2, etc., until the entire velocity history had been determined. Figure 9 thus shows how a large excursion on a data trace maps into a small percentage of the total excursion in velocity. If F_{max} is the total number of fringe oscillations corresponding to the peak surface velocity, it can be seen from Fig. 9 that the total excursion in velocity is broken down into $4F_{max}$ high-resolution velocity increments which are obtained from the two 90°-out-of-phase oscillograms. Thus, the iron experiment velocity history of Fig. 6 is a composite of over 16 high-resolution velocity increments. The influence of the oscillogram noise on the velocity data is therefore greatly demagnified.

The rise time of the system was limited largely by the 50-MHz frequency response of the dual-beam recording oscilloscopes. Very significant improvements in rise time can be made by using faster oscilloscopes and photomultiplier tubes. These improvements are also under consideration. Note in Fig. 3 that the interferometer produces two signal beams, one going to the right and one to the left of the large beam splitter. The left-hand signal beam, which is not used at present, could be sent through a second polarizing beam splitter, and the two resulting 90°-out-of-phase signals could be used with a very fast photomultiplier and oscilloscope recording system. This could better define the rise times of shock fronts, for example, while still using the rest of the system for the accurate measurement of the longer-term aspects of the velocity history.

There is an inherent rise time in the output of the velocity interferometer itself which has the effect of averaging the velocity over the delay time τ.[13] Although there are data-reduction techniques which can decrease the response time of the reduced data to less than τ,[12,14] the simplest way of decreasing the rise time is to reduce τ itself. The VISAR has a distinct advantage here, since the delay times are quite short. The VISAR used for the data presented in this paper has a maximum delay time of only 1.5 nsec.

The specimen surface tilt and a depth-of-field effect can be two further sources of error. Their magnitudes are related to the degree of imperfection of the optics in the interferometer portion of the VISAR. When the interferometer has been aligned for an experiment, certain paths are taken by the laser light in going through the optics in the interferometer. If the light paths change during the time of data collection, and if the optics are not perfect, then a fringe shift due to the change in the optical path through the interferometer may be superimposed upon the desired fringe data.

One of the main causes of a change in the optical path in a shock-wave experiment might be a tilting of the specimen surface during its motion. When a spectral specimen surface is used, the light reflected from the surface falls onto some small part of the lens L (Fig. 4). The subsequent path through the rest of the optics depends slightly upon the location at which the reflected beam passes through the lens. This location, of course, is a function of the tilt of the specimen surface. Experiments with the present VISAR have indicated that a spectral specimen surface tilt of 0.1° can produce a fringe shift error of about 0.01 fringe. Tilts of less than 0.1° are attainable in most shock experiments.

One would expect the optical path to remain essentially unchanged even for several degrees of tilt whenever the specimen surface is a Lambert diffuse reflector, for in this case all of the lens L is uniformly illuminated by the reflected light at all times, regardless of the tilt. However, although the original alignment of the VISAR calls for the specimen surface to be at the focal point of the lens L, the surface begins to move away from its ideal location as soon as the motion starts. When this occurs, the lens no longer exactly recollimates the reflected light. This causes the diameter of the beam through the interferometer to vary during the motion, which again represents a change in the optical path. The magnitude of the fringe count error resulting from this finite depth-of-field effect was also investigated by experiment. Using the configuration of the iron experiment (Fig. 4), it was found that the specimen surface motion caused a fringe shift of no more than 0.02 fringe per mm of displacement. Since there were slightly more than four fringes in the iron experiment, and since the surface moved only about 1.2 mm during the period of observation, the depth-of-field error was probably less than 0.6%.

It is interesting to estimate roughly how the depth-of-field error varies with the diameter and the focal length of the lens L. As the distance between the surface and the lens decreases, the light transmitted through the lens ceases to be collimated and becomes more and more divergent. It seems reasonable to assume that the depth-of-field error is proportional to the angle of divergence of the light transmitted through lens L. If E is the depth-of-field error, a simple calculation indicates that

$$E \propto r\Delta x/f^2, \quad \Delta x \ll f$$

where r is the lens radius, f is its focal length, and Δx is the distance moved by the specimen surface. In the iron experiment, r was 25 mm and f was 300 mm. These values, together with the experimentally determined fringe shift of 0.02 fringe per mm, allow the proportionality constant for the above expression to be evaluated. If ΔF represents the error in the fringe count, we find that

$$|\Delta F| < 75 r\Delta x/f^2.$$

A much more powerful laser will provide sufficient light to allow f to be doubled or tripled while keeping r constant. This will greatly enhance the depth-of-field capability in shock experiments.

A depth-of-field effect also applies to the case of a spectral specimen surface, but the effect will generally be smaller because the reflected beam usually passes through the lens at a radius of $\frac{1}{2}r$ or less. This advantage of the spectral reflector is countered by the greater sensitivity to light path changes due to specimen surface tilt.

With a given VISAR design, one will have a "built-in" error factor which is determined by the degree of perfection of the optics and by the maximum possible delay time τ. In order to obtain 2% accuracy with the present design, the peak velocity to be measured should correspond to a fringe count of at least one fringe, such that the errors from noise and nonlinearities, for example, are effectively demagnified. Thus, the minimum velocity for 2% accurate data is at present about 0.2 mm/μsec. Much smaller velocities can be measured, of course, but the uncertainty of the measurement will increase correspondingly.

VI. CONCLUSIONS

The VISAR still requires light of high temporal coherence, but spatial coherence is not necessary for good fringe contrast. Thus, single-frequency laser light can be reflected from any moving surface, whether spectral, diffuse, or neither quite one nor the other, and the VISAR can detect the Doppler shift of the reflected light. The VISAR is especially insensitive to tilt when operated with a diffuse specimen surface. It can be used in a very large depth-of-field mode, such that the velocity history of a projectile accelerating through a 4-m gun barrel can be measured, for example. The VISAR allows very accurate laser interferometry to be applied to a large range of situations which were difficult or impossible to instrument with previous techniques.

ACKNOWLEDGMENT

The authors greatfully acknowledge very helpful conversations with C.W. Gillard whose consultation contributed to the early phase of the VISAR development.

---

*Work supported by the U. S. Atomic Energy Commission.

[1]L. M. Barker, Exp. Mech. **12**, 40 (1972).
[2]L. M. Barker and R. E. Hollenbach, J. Appl. Phys. **41**, 4208 (1970).
[3]L. M. Barker and R. E. Hollenbach, Rev. Sci. Instrum. **36**, 1617 (1965).
[4]H. H. Zwick and G. G. Shepherd, Appl. Opt. **10**, 2569 (1971).
[5]G. Hansen, Z. Instrumentenk. **61**, 411 (1941).
[6]R. L. Hilliard and G. G. Shepherd, J. Opt. Soc. Amer. **56**, 362 (1966).
[7]C. W. Gillard, U.S. Patent No. 3 503 012 (unpublished).
[8]C. W. Gillard, G. S. Ishikawa, J. E. Peterson, J. L. Rapier, J. C. Stover, and N. L. Thomas, Lockheed Report No. N-25-67-1, 1968 (unpublished).
[9]C. W. Gillard (private communication).
[10]G. M. B. Bouricious and S. F. Clifford, Rev. Sci. Instrum. **41**, 1800 (1970).
[11]D. Barncraft, E. L. Peterson, and S. Minshall, J. Appl. Phys. **27**, 291 (1956).
[12]R. J. Clifton, J. Appl. Phys. **41**, 5335 (1970).
[13]L. M. Barker, in *Behavior of Dense Media Under High Dynamic Pressures* (Gordon and Breach, New York, 1968), p. 483.
[14]L. M. Barker, Rev. Sci. Instrum. **42**, 276 (1971).